Bockris, J., et al. *Does Tritium Form at Electrodes by Nuclear Reactions?* in *The First Annual Conference on Cold Fusion*. 1990. University of Utah Research Park, Salt Lake City, Utah: National Cold Fusion Institute.

DOES TRITIUM FORM AT ELECTRODES BY NUCLEAR REACTIONS?

J. O'M. Bockris, G.H. Lin, R.C. Kainthla,
N.J.C. Packham and O. Velev

Surface Electrochemistry Laboratory
Texas A&M University
College Station, TX 77843

ABSTRACT

This paper reports tritium formed in LiOD D_2O solutions in which Pd cathodes are used to evolve D_2. Electrolysis was carried out for up to 4½ months. Excess heat has been observed from 5 electrodes out of 28, tritium in 15 out of 53 but 9 out of 13 if the electrodes are limited to 1 mm diameter. Steady state tritium concentrations were 10^4-10^7 disintegrations min^{-1} ml^{-1}. A weak correlation may exist between heat observed and tritium produced. The rate of production of tritium was c. 10^{10} atoms cm^{-2} sec^{-1}. The branching ratio of tritium to neutrons was ~ 10^8.

A theoretical dendrite enhanced fusion model is suggested. Growing gas layer breakdown occurs at sufficiently high surface potential dendrite tips and correspondingly fusion reactions occur. The model gives quantitative consistence with experiment, especially the sporadic nature and the observed branching ratio.

INTRODUCTION

Since Fleischmann, Pons and Hawkins [1] and Jones [2] reported the cold fusion phenomena, which is difficult to explain by conventional nuclear physics, several attempts to interpret the excess heat as well as radiative particle emission have been made. Such explanations fall into two large categories: chemical reaction and nuclear fusion. The heat released by a chemical reaction corresponds to the range of a few electron volts (eV) per atom in contrast to the energy liberated in a nuclear reaction – on the order of millions of electron volts (MeV) per nucleus. In an earlier paper [3], we summarized the eight possible chemical contributions to the excess heat seen in reference 1, and arrived at the conclusion that any chemical explanation would be improbable. No one chemical explanation will suffice to explain the magnitude of the excess heat observed, and the large amount of tritium produced in the solution and gas phases [4,5] cannot be explained by any kind of chemical reaction. The second category of explanation is a nuclear one. Different models [6-9] to explain the cold fusion experiments have been suggested since they cannot be simply interpreted by today's nuclear physics. In a review paper [10], different fusion experiments and theoretical explanations have been summerized.

There are two main characteristics of the cold fusion experiments. One is the large tritium to neutron ratio, on the order of 10^8, and the other is the sporadicity and irreproducibility of the phenomena. A suitable cold fusion theory or model must explain both of these two features.

A large amount of tritium has been observed both in the solution and gas phases in this laboratory, which cannot simply be explained by isotopic enrichment. The maximum tritium concentration in the solution due to isotopic separation at infinitely long times, is about 2 times the tritium concentration in the original solution [5], which is very small compared to the experimental results.

EXPERIMENTAL

(a) Sources of Electrode Materials

The 1mm and 3mm Pd cathodes used in the present study were cut from 99.9% pure rods made by Hoover and Strong, Richmond, VA and purchased from the Texas Coin Exchange, College Station, while the 6mm diameter electrodes were cut from the 99.9% pure rod purchased from Sure Pure Chemicals, NY. The 4mm cathodes were cut from high purity "fusion" Pd on loan from Johnson Matthey. The lengths of the electrodes were cut about 4cm, 3cm, 2.5cm and 2.5cm, respectively.

Pt electrodes were of 99.9% purity, from Alfa Products, Danvers, MA, titanium (99.99%), from Johnson Matthey, Seabrook, NH, and Ni gauze (99.9%), from the Belleville Metals Company, Belleville, NJ.

99.9% pure D_2O was obtained from Aldrich Chemical Co.

(b) Pre-treatment

After cutting to appropriate sizes, the electrodes were pre-treated. This involved either: no pre-treatment, acid etching, annealing, electrochemical, hammering, electrodeposition of Pd, electroless deposition of Pd.

(c) Charging

After pre-treatment, a Ni wire was spot welded to the electrode, and put into small electrolytic cells with appropriate electrolyte and counter electrodes (Table 1).

The cells were then put on a charging current of ~64 mA cm^{-2} while the cell voltage was ~3.0-4.0 V. The cells were refilled with D_2O for a few weeks to a few months. Sometimes, the Ni anode was repaired or replaced along with the solution and the glass tube.

(d) Heat Measurements

After charging, for times varying from 10-25 weeks, the electrodes were transferred to a calorimeter for the measurement of heat.

The calorimeter used in the study was of the heat transfer type, and has been described elsewhere [11].

(e) Tritium Measurements

Tritium analysis was performed on the alkaline electrolyte by in-situ Liquid Scintillation Counting (LSC). Multiple blank samples of H_2O, D_2O, and 0.1 M LiOD were included for analysis. A test for chemiluminescence was made using samples ranging from 1M to 1M LiOD, including samples that had been neutralized by potassium hydrogen phthalate. Results are shown in Fig. 1. One minute and ten minutes analyses (some samples were run overnight) were performed. A detailed analysis of the energy spectra from the Cyclotron Institute counters yielded the correct β energy end point for tritium (18keV) c.f. Figs. 2a and 2b.

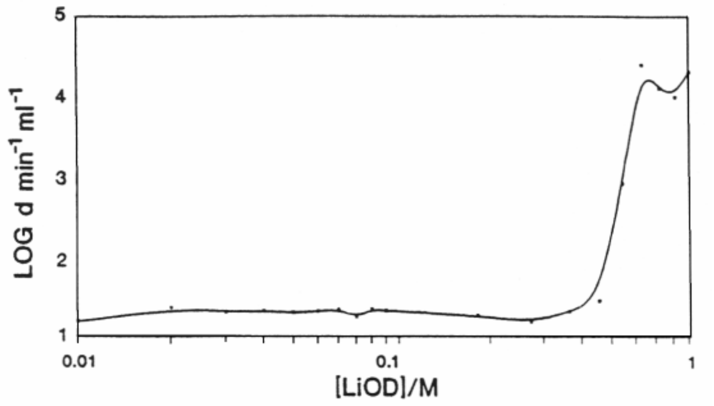

Fig. 1. The effect of electrolyte concentration on chemiluminescence of the scintillation cocktail [4].

The results are shown in Table 2. The tritium content of the liquids resulting from the electrolyses, including a tritium (HTO) standard and blanks of LiOD and D_2O, was examined by Los Alamos National Laboratory, Argonne National Laboratory, Battelle Pacific Northwest Laboratory and the General Motors Research Laboratory. These results are shown in Table 3.

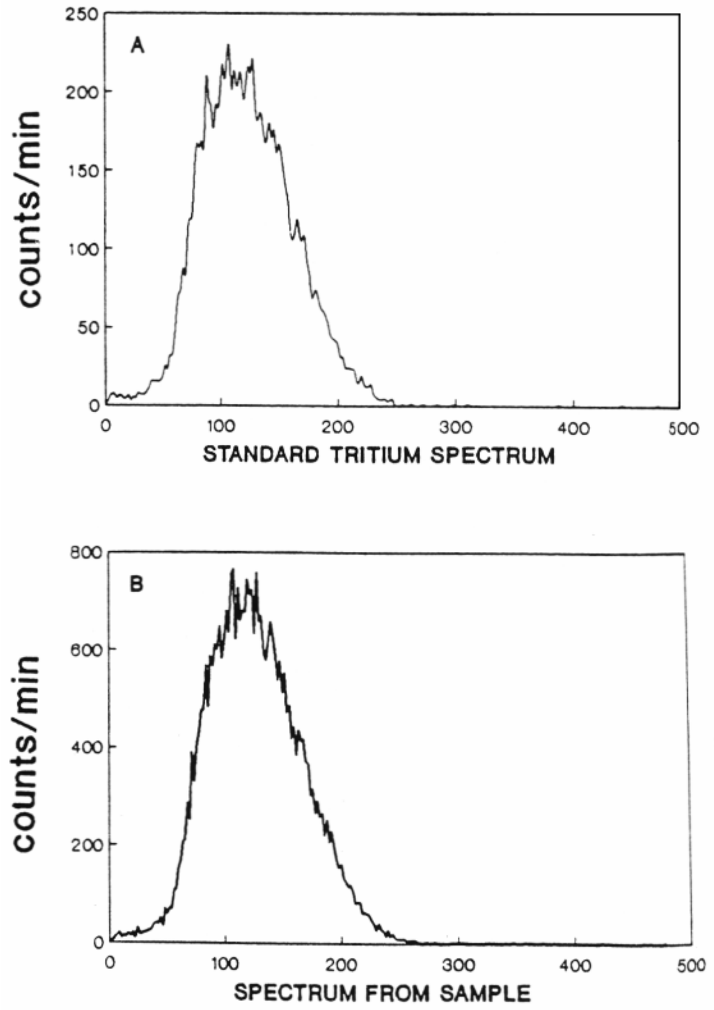

Fig. 2. (a) The spectrum of a tritiated water sample.

TABLE 1. SPORADIC OBSERVATIONS OF TRITIUM AND HEAT DURING D_2 EVOLUTION FROM D_2O ON PD

CELL	ELECTRODE PRETREATMENT	SOLUTION	TRITIUM	EXCESS HEAT
A1 (1mm)	No treatment	0.1M LiOD	Yes	NM
A2 (1mm)	No treatment	0.1M LiOD + 0.1mM NaCN	Yes	NM
A3 (1mm)	Annealed, 800°C, 6 hrs	0.1M LiOD	Yes	NM
A4 (1mm)	Annealed, 800°C, 6 hrs	0.1M LiOD + 0.1mM NaCN	Yes	NM
A5 (1mm)	Acid Etch	0.1M LiOD	Yes	NM
A6 (1mm)	Acid Etch	0.1M LiOD + 0.1mM NaCN	Yes	NM
A7 (1mm)	Electrochemical	0.1M LiOD	Yes	NM
A8 (1mm)	Electrochemical	0.1M LiOD + 0.1mM NaCN	Yes	NM
A9 (1mm)	No treatment, charged in U tube	0.1M LiOD	No	Yes
M1 (1mm)	No treatment	0.1M LiOD	Yes	NM
M2 (1mm)	Acid Etch	0.1M LiOD	No	NM
B1 (3mm)	No treatment	0.1M LiOD	No	No
B2 (3mm)	No treatment	0.1M LiOD + 0.1mM NaCN	No	No
B3 (3mm)	Annealed, 800°C, 6 hrs	0.1M LiOD	Yes	No
B4 (3mm)	Annealed, 800°C, 6 hrs	0.1M LiOD + 0.1mM NaCN	No	No
B5 (3mm)	Acid etch	0.1M LiOD	No	No
B6 (3mm)	Acid etch	0.1M LiOD + 0.001M NaCN	No	No
B7 (3mm)	Electrochemical	0.1M LiOD	No	No
B8 (3mm)	Electrochemical	0.1M LiOD + 0.001M NaCN	No	Yes
B9 (3mm)	No treatment, charged in U tube	0.1M LiOD	No	Yes
C8 (6mm)	Electrochemical	0.1M LiOD + 0.001M NaCN	No	No
CELL 1 (6mm)	No treatment	0.1M LiOD	No	No
CELL 4 (3mm)	Annealed, 1200°C, 12 hrs	0.1M LiOD	Yes	Yes
JM1 (4mm)	No treatment	0.1M LiOD	No	No
JM2 (4mm)	Annealed, 800°C, 24 hrs	0.1M LiOD	No	No
CELL 4A (3mm)	No treatment	0.1M LiOD	No	No
H1 (3mm)	Hammered; Electrochemical	0.1M LiOD	No	No
AH1 (3mm)	Annealed, 800°C, 8 hrs Hammered, Electrochemical	0.1M LiOD	No	No
Cell 1A (6mm)	Annealed, 800°C, 8 hrs	0.1M LiOD	No	No
Cell 1B (3mm) on Pd	Electrodeposited Pd	0.1M LiOD	No	No
B5A (3mm)	Annealed, 800°C, 24 hrs	0.1M LiOD	No	No

NM = No attempt made to measure.

TABLE 2. CELL IDENTIFICATION, ELECTRODE TREATMENT, SOLUTION TYPE AND TRITIUM ACTIVITY OF ELECTROLYTE SAMPLES PERFORMED ON 1219 LSC

CELL	ELECTRODE PRETREATMENT	SOLUTION	CORRECTED ^{3}H ACTIVITY (dpm/ml^{-1})
A1	No treatment	0.1M LiOD	3.8×10^4
A2	No treatment	0.1M LiOD + 0.1mM NaCN	
	After 16 days at 50 mA cm^{-2} then for 8 hours at 500 mA cm^{-2} (5/1/89)		168
	50 mA cm^{-2} for 4 days (5/5/89)		134
	50 mA cm^{-2} for 3 hours, 110 mA cm^{-2} for 2 hours, 200 mA cm^{-2} for 20 minutes (5/6/89)		1.1×10^4
	50 mA cm^{-2} (5/7/89)		1.4×10^4
	(5/7/89 - 5/13/89)		1.1×10^4
	(5/13/89 - 6/6/89)		7.5×10^3
A3	Anneal	0.1M LiOD	4.9×10^6
A4	Anneal	0.1M LiOD + 0.1mM NaCN	1.2×10^5
A5	Acid Etch	0.1M LiOD	3.7×10^6
A6	Acid Etch	0.1M LiOD + 0.1mM NaCN	3.3×10^4
A7	Electrochemical Before high current density	0.1M LiOD	102
	After 2 hours at 500 mA cm^{-2}		5223
	After 6 hours at 500 mA cm^{-2}		5.0×10^5
	After 12 hours at 500 mA cm^{-2}		7.6×10^5
A8	Electrochemical After 16 days charging and 8 hours high current density (5/1/89)	0.1M LiOD + 0.1mM NaCN	192
	Electrolyte levels after 6 weeks at 50 mA cm^{-2}		5.0×10^5
	Recombined gas levels after 2 weeks of external recombination at 50 mA cm^{-2}		5.0×10^7
B3 (3mm)	Anneal	0.1M LiOD	6.3×10^4
B5 (3mm)	Acid Etch	0.1M LiOD	48
CELL 1 (6mm)	No treatment	0.1M LiOD	117
CELL 4		See Fig. 5	
M1	No treatment	0.1M LiOD	3000

TABLE 3. CONFIRMATORY RESULTS FROM OUTSIDE SOURCES ON VARIOUS SAMPLES CORRECTED ^{3}H ACTIVITY IN dpm/ml^{-1}

SAMPLE	CELL 1	CELL 2	HTO STANDARD	0.1M LiOD	D_2O
INSTITUTION					
Texas A&M	2.13 × 106	1157	7.23 × 105	93	47
Battelle	1.96 × 106	1170	8.08 × 105	127	140
Argonne	1.96 × 106	1020	7.59 × 105	90	114
Los Alamos	1.97 × 106	800-1300	6.50 × 105	113	161
General Motors	1.80 × 106	1000	------	NOT ANALYZED	------

(f) Contamination

The possibility that large amounts of tritium were present in either the D_2O or the Li used to make the LiOD, is ruled out by the Results of Tables 4a and 4b. Each batch of D_2O that was used for refilling the cells was analyzed for tritium content, both on the 1219 instrument (Table 4a), and the 1410 (Table 4b, shown as a mean of 10 results). Many experiments were run in which no significant increase of tritium was observed, including identical cells to the ones which did produce tritium, except for the electrolyte, which was 0.1M LiOH in H_2O (Tables 4b and 5). Possible contamination from the nickel anode was examined by neutralization and then counting, with negative results.

Virgin palladium and nickel of the same batch used for all 1mm Pd cells were sent for analysis to LANL with no tritium being detected.

If it is supposed that the Pd had, earlier in its history, suffered prolonged exposure as a cathode in D_2O, T would have diffused into the electrode. Simple calculation shows [12] that it would take $<10^2$ hours to diffuse out again for a Pd rod kept in air.

Finally, some of the electrodes which gave tritium had been heavily annealed just prior to immersion in the D_2O-LiOD. Thus, contamination would seem unlikely.

EXPERIMENTAL RESULTS

1) Reproducibility and Repeatability

The special difficulty of the present work is poor repeatability. Table 1 summarizes some of the results of heat and tritium measurements on all the electrodes studied so far in this laboratory. Excess heat has been observed in only 5 out of the 28 electrodes, tritium in 15 out of 53. The observation of tritium with 1mm diameter wires has been more successful with 9 out of 13 1mm electrodes yielding tritium. None of the seven 6mm electrodes have shown any excess heat or tritium for observation periods of up to 6 months. Both heat and tritium has been observed together only for one electrode. However, in some half of the present work, heat and tritium were not regularly recorded together. Further, heat and tritium come in bursts. T may have been produced during some heat bursts (as DT) and sparged out before measurement was be made. The duration of the experimental work covered in this paper is about 25 weeks.

2) Rise Times during Switch-on

In one of the cells (cell A7 c.f. Table 2) the build up of tritium as a function of time was followed at high current density. The results shown in Fig. 3 indicate either the time for reaching equilibrium of DT in solution to DT in the gas over the solution; or represent the time in which a burst occurred, the product being largely DTO.

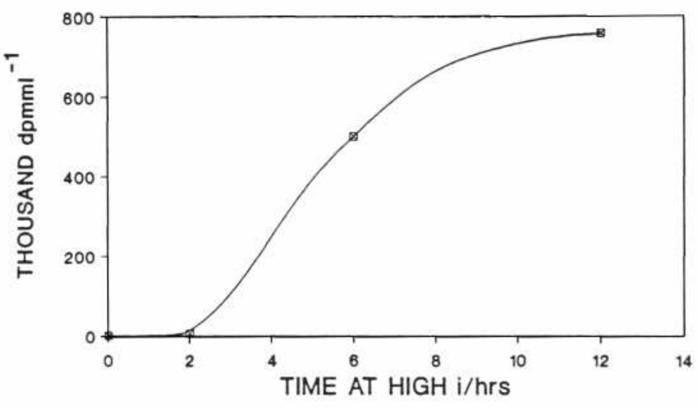

Fig. 3. The production of tritium in the electrolyte of cell A7 as a function of time [4].

3) Fall Time during Switch-off

Another cell (cell A2 in Table 2) was tested for tritium over an extended period of time. It was run at a low current density for 16 days, followed by a 10 hour period at high current density, after which, tritium was not produced. The cell was then transferred to the Cyclotron Institute where it remained at low current density for another week, with no tritium production. On May 6, the current was increased to 110 mA cm^{-2} for two hours, increased again to 300 mA cm^{-2} for 20 minutes, decreased to 90 mA cm^{-2} for seven days then returned to 50 mA cm^{-2} until June 22. The tritium content of the solution was monitored during this time and the results are shown in Fig. 4, which indicates the production period was about 2 days, and the decay period about 3 days.

4) The Steady State Tritium Values

The steady state concentrations in T producing cells varied between 10 and 5×10^6 dpm/ml^{-1}. These are shown in Table 2. The tritium production rate is 2×10^8 - 2×10^9 atoms sec^{-1} for the first and second bursts in the experiment, respectively. The maximum rate we observed is about 10^{10} atom sec^{-1}.

TABLE 4a. BLANK EXPERIMENTS DURING TRITIUM ANALYSIS PERFORMED ON THE 1219 COUNTER

SAMPLE	cpm/ml^{-1}	BACKGROUND CORRECTED ACTIVITY (dpm/ml^{-1})
D_2O Analysis #1	65	48
D_2O Analysis #2	70	63
D_2O Analysis #3	67	54
D_2O Analysis #4	60	33
D_2O Analysis #5	50	3
D_2O Analysis #6	71	66
D_2O Analysis #7	75	78
D_2O Analysis #8	62	39
0.1M LiOD Analysis #1	75	78
0.1M LiOD Analysis #2	70	63
0.1M LiOD Analysis #3	74	75
0.1M LiOD Analysis #4	65	48
0.1M LiOD Analysis #5	60	33
0.1M LiOD Analysis #6	66	51
0.1M LiOD Analysis #7	76	81
0.1M LiOD Analysis #8	70	63
Neutralized 0.1M LiOD	73	72
Neutralized 0.1M LiOD + 0.1mM NaCN	76	81
Dissolved nickel in acid Analysis #1	78	87
Dissolved nickel in acid Analysis #2	80	93
Dissolved nickel in acid Analysis #3	76	81
Scintillation cocktail	49	--

TABLE 4b. MEAN OF 10 BLANK EXPERIMENTS DURING TRITIUM ANALYSIS PERFORMED ON THE 1410 COUNTER

SAMPLE	cpm/ ml^{-1}	BACKGROUND CORRECTED ACTIVITY (dpm/ml^{-1})
BIOSAFE II COCKTAIL	170±13	--
H_2O Analysis	161±16	0
D_2O Analysis	210±16	100
0.1M LiOD Analysis	220±20	125
0.1M LiOH Analysis	157+12	0
Dissolved Nickel in Nitric Acid	140±20	0
Tygon Tubing in NaOH	105±20	0
Rubber Stoppers in NaOH	150±20	0
Recombination Catalyst in NaOH	140±15	0
Dissolved Shavings from Cutters	160±11	0
Dissolved Shavings from Vacuum Chamber	164±17	0
Dissolved Shavings from Spotwelder	155±10	0

5) Pre-treatment and Degree of Tritium Production

Details on the pretreatment of the electrodes that produced tritium are given in Table 1.

The cell 4 electrode, the only electrode which has shown excess heat twice and two tritium bursts, was vacuum annealed at 10^{-6} torr at 1200-1300°C for 12 hrs. The excess heat was observed for the first time after about 3.5 months, while the combined tritium and excess heat were observed after about 4.5 months of electrolysis.

Correlation of Tritium Production to Heat

Some relation between heat and tritium production is indicated qualitatively by the shape of the relation shown in Fig. 5.

Branching Ratio

The tritium production rate is about 10^9 atoms sec^{-1} cm^{-2} from our experiments. Neutron bursts have been observed by Wolf et al. [13], at the level of 1 to 2 sec^{-1} cm^{-2}. Thus, the branching ratio is on the order of 10^9. However, other results [14,15], show that the neutron production rate may be about 10^2 sec^{-1} cm^{-2}. Thus, on this basis, the branching ratio would be ~10^7.

FUSION MODELS

In Fig. 6, the take-off time for the growth of promontories occurs at times between 2 and 100 days for assumed impurity concentrations in the range 10^{-7} - 10^{-5} M. It is the time at which rapid increase of dendritic growth begins which fixes the time at which the production of tritium commences. The “Impurity” is likely to be the anode material but a surprising number of metals on the cathode have been observed after prolonged electrolysis [16]. These are the most likely places where high electric fields or high stress fields may develop which make fusion more probable.

Such a hypothesis is consistent with the sporadicity of the effects, and the variety of the nature of the cathode deposits. Large electrodes would tend not to produce tritium. Their surface area getters the solution of impurities before the transition time for rapid dendrite growth has been reached.

The electric field in the double layer at an electrode is usually taken as having an order of magnitude of 10^8 V cm^{-1}. However, recently Kolb and Franke [17] have concluded that it can be ~ 10^9 V cm^{-1} in certain areas. The enhancement is due to surface states on the electrode which concentrate the field lines near these states.

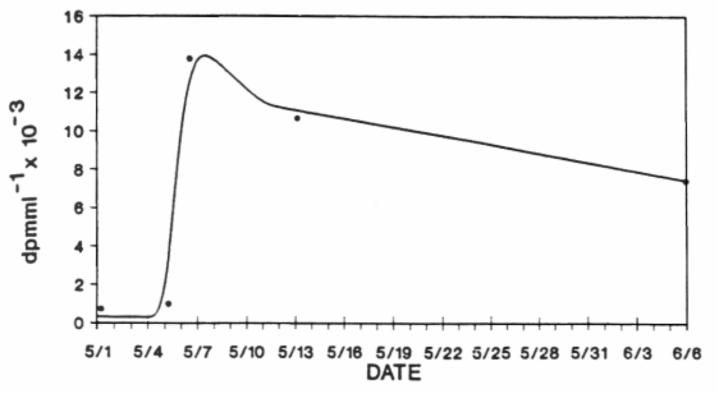

Fig. 4. The production of tritium in the electrolyte of cell A2 as a function of time (ordinate gives date) [4].

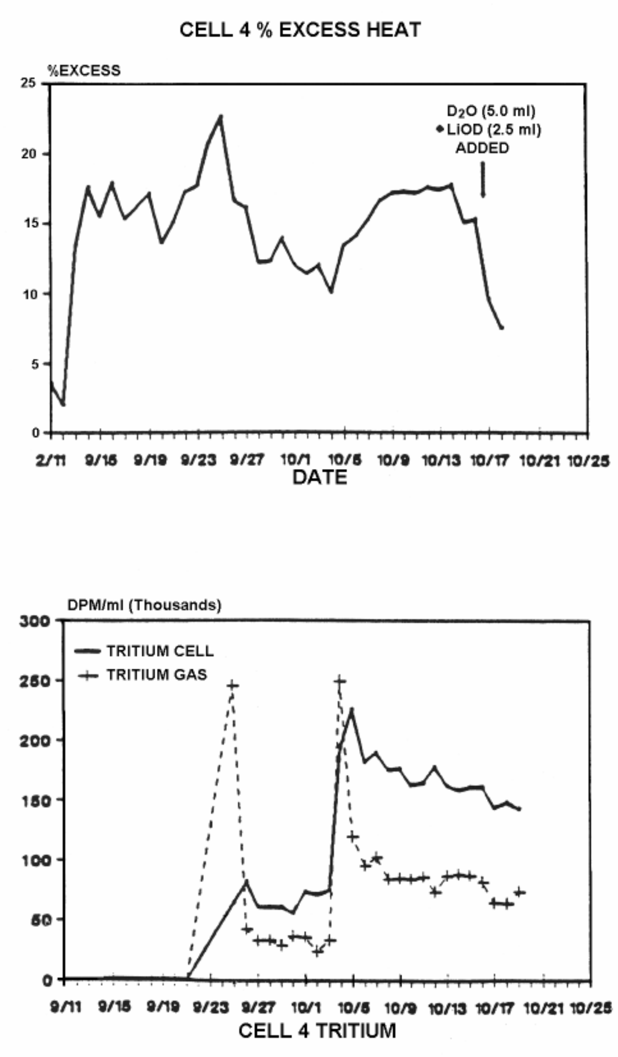

Fig. 5. The heat measurements and tritium activity levels from cell 4 showing a possible correlation between the two.

TABLE 5. DETAILS OF CELLS THAT PRODUCED NO TRITIUM WITH 1410 LSC (CORRECTED ACTIVITY)

EXPERIMENT	dpm/ml^{-1}
3mm × 3cm Ti Cathode in 0.1M LiOD with internal gas recombination	275
3mm × 3cm Pd Cathode in 0.1M LiOD with internal gas recombination	235
3mm × 3cm Ti Cathode in 0.1M LiOD with internal gas recombination	285
0.5mm × 1cm Pd Cathode in 0.1M LiOD with internal gas recombination	55
4mm × 2mm Pd disc Cathode in 0.1M LiOD with internal gas recombination	365
0.5mm × 1cm Pd Cathode in 0.1M LiOD with external gas recombination (recombined gases measured)	315
1mm × 4cm Pd Cathode in 0.1M LiOD with external gas recombination (recombined gases measured 7/18/89)	75
1mm × 4cm Pd Cathode in 0.1M LiOD with external gas recombination (recombined gases measured 7/21/89)	33
1mm × 4cm Pd Cathode in 0.1M LiOH (H_2O) No gas recombination	0
1mm × 4cm Pd Cathode in 0.1M LiOH (H_2O) N gas recombination	18

TABLE 6. THE RELATIONSHIP BETWEEN REQUIRED ENERGY AND THE FUSION RATE, f

E (eV)	G	f(i=lA/cm^2)	fΓ (i=1A/cm^2)
1000	2.63×10^{-14}	1.64×10^{5}	1.64×10^{2}
1500	8.18×10^{-12}	5.11×10^{7}	5.11×10^{4}
2000	2.50×10^{-10}	1.56×10^{9}	1.56×10^{6}
2500	2.59×10^{-9}	1.61×10^{10}	1.61×10^{7}
3000	1.44×10^{-8}	9.00×10^{10}	9.00×10^{7}
3500	5.52×10^{-8}	3.45×10^{11}	3.45×10^{8}
4000	1.62×10^{-7}	1.01×10^{12}	1.01×10^{9}

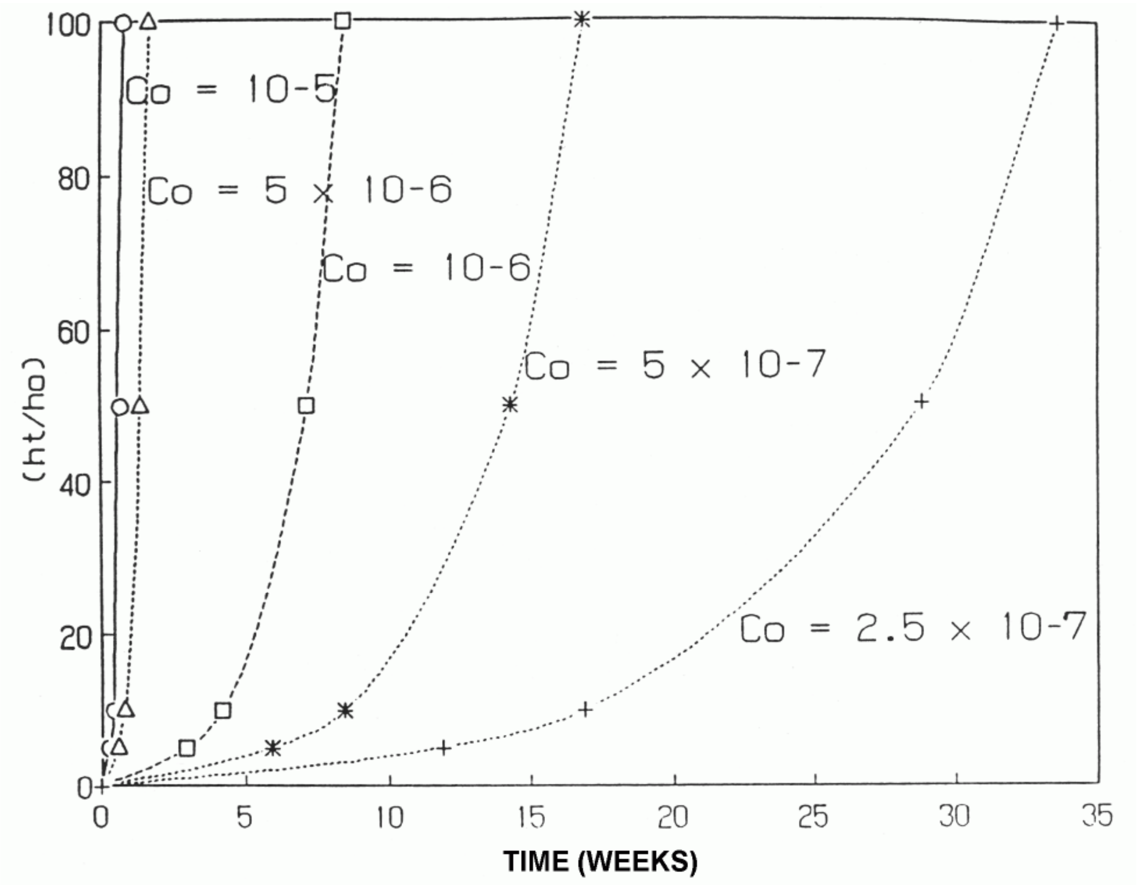

Fig. 6. The growth of promontories on the surface of electrodes as a function of time and impurity concentration.

The tips of dendrites are the points at which local dielectric breakdown is likely. It seems reasonable to accept values for the local double-layer field of > 10^9 volts cm^{-1}. There is no simple method of calculating the enhancement in field due to the dendrite tip. It will therefore be assumed (somewhat conservatively) that this serves to double the large values of the field deduced by Kolb and Franke [17].

The breakdown of the water dielectric is likely to begin at sharp points (i.e. the dendrite tips) on the electrode surface, and thereafter a D_2 gas layer will be formed at the surface [18] (Fig. 7). When the gas layer grows, a transient large electric voltage drop may be developed on the dendrite tips. Electron emission will occur from dendrite tips into the gas, and in the gas layer the breakdown reaction:

$$D_2 + e_o \rightarrow D^+ + D + 2e \tag{1}$$

seems feasible. Indeed, dark blue sparks have been seen in certain electrolyzing cells.

The D^+ produced will be pulled by the field lines through the gas to the cathode surface on the nearest available surface, the dendrite tip. Such a surface will be likely to retain adsorbed D with which the D^+ would be expected to collide.

The D^+ path length may be of the order of the thickness of the gas layer, c. 100 Å. Hence, the transient voltage drop would be about 2000 eV.

Suppose i is the current density in amps cm^{-2}, then N_Ai/F is the number of D-D collisions on the electrode surface [1] in atoms cm^2 sec^{-1}, where F is the charge on one gram ion, in coulombs.

Let it be supposed that a fraction, Γ of the surface is occupied with sharpened tip material. Then, let the probability of tunneling at such places be P_T, equivalent to:

$$P_T = \exp\{-\pi e_o^2 M^{½}/\hbar E^{½}\} \tag{2}$$

Therefore, the rate of T formation in atoms sec^{-1} cm^{-2} is given by:

$$\Gamma\ i/F\ P_T \tag{3}$$

In Table 6, this function is tabulated for i = 1 amp cm^{-2} and $\Gamma = 10^{-3}$. It is seen that the calculated fusion rate is about 2×10^6 compared with the experimental rate of 10^8 to 10^{10} atoms cm^{-2} sec^{-1}.

Quantitative agreement with the model can be obtained by doubling the field to allow for its concentration at a sharp point. The assumption that Γ might be ~ 10^{-3} is based on the appearance of the electron microscope pictures of Pd electrodes after prolonged electrolysis. It is possible that $\Gamma < 10^{-3}$, reducing the degree of agreement.

On the other hand, quantitative treatments of two factors neglected in this first approach would tend to increase the rate.

(i) The double layer involves electron overlap [19]. The electron cloud existing at the tip of the dendrite acts as a screen and reduces repulsion. Correspondingly, the adsorbed deuteron is shielded by the loss of cationic character. Recently, Kim [20] has shown that electron screening may greatly reduce the needed collision energy. Hence, it would be possible to dispense with the reliance on the specially high electric fields arising from the work of Kolb and Franke and use those normally seen by electrochemists, i.e. 10^8 volts cm^{-1}.

(ii) Worledge et al. [9] have suggested that the effective mass of the deuteron is less than the rest mass in a force-free field. On this basis, the needed E in Gamow expression declines in proportion to the reduction of M_D. At $M_D = 0.01$, 4×10^7 volts cm^{-1} would give agreement with experiment and this is generally available in the electrical double layer at electrodes without the enhancement arising from low radius dendritic tips.

In the plasma nuclear fusion, two deuterons collide with a random orientation, the two product channels, helium and neutrons or tritium and hydrogen, have almost the same probability. However, at the electrode, the deuteron, during its acceleration across the thin gas layer, will be subject to a vectorial force which will cause it to orient preferentially. One of the two branches will then be favored.

The deuteron is known to be a loosely bound entity, the wave function of which may effectively extend to 20 fermi. When a deuteron is incident on the surface, it feels a strong negative electric field (~2×10^9 V cm^{-1}) because of the pure negative excess surface electric charge. The electric field leads to an effective polarization of the deuteron or a p-wave component term in the deuteron's internal wavefunction. However, when this deuteron is close to the classical turning point, it will experience a strong positive electric field (> 10^{12} V cm^{-1}). This field forces the incident deuteron to reverse its orientation in a specific manner. The deuteron

---

[1] The collisions arise in the Volmer-Heyrovsky mechanism due to D_2O discharging a proton onto an adsorbed D to give D_2.

would gain the energy in such a fast reversal of the electric field. Then, the angular momentum of the incident deuteron may be excited from the J=0 state to J=2 or even partly to J=4 states. This fast (~ 10^{-17} sec) reversal of orientation may cause an induced porolization and loosen the structure of the deuteron nucleus, which may create a condition favor to Philips-Oppenheimer type stripping reaction – the tunneling neutron transfer reaction $D + D \rightarrow T + P$ [21]. The reasons for this kind of stripping reaction are (1) the orientation may help the neutron transfer process; (2) the proton transfer reaction has to penetrate an extra Coulomb barrier compared to the neutron transfer process.

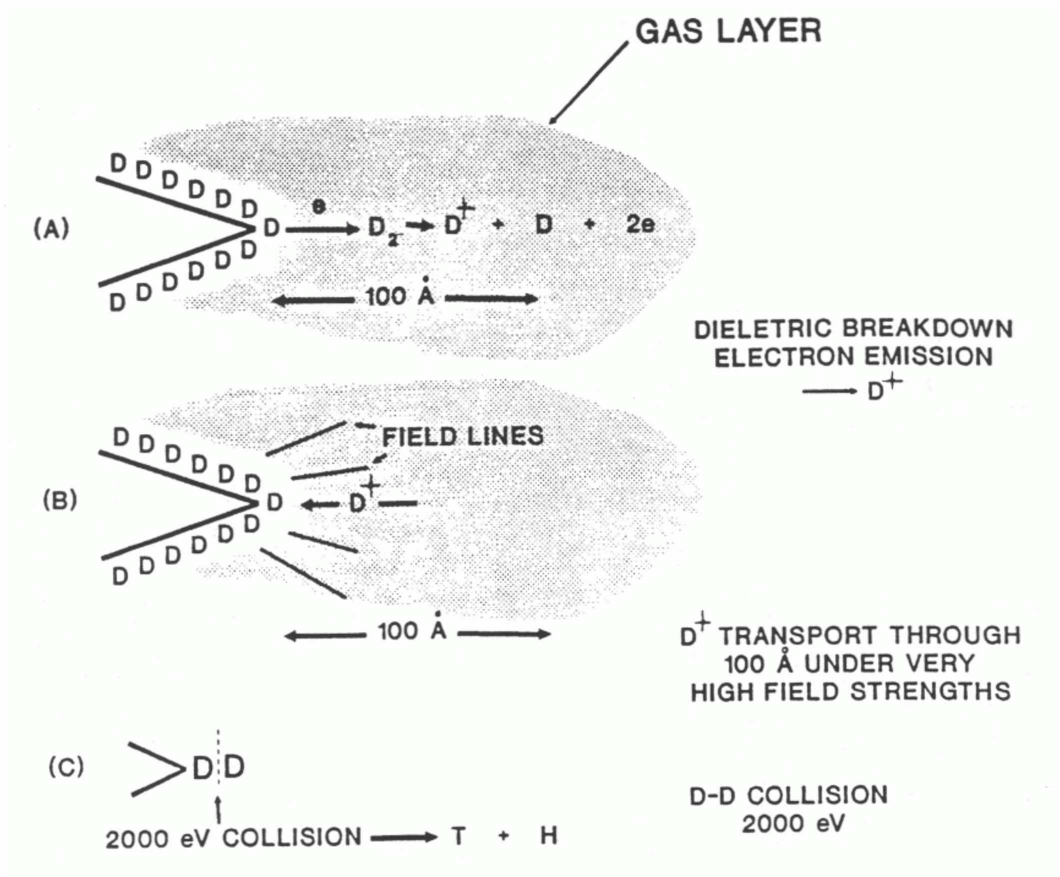

Fig. 7. Dielectric breakdown on a gas covered dendrite tip.

The smaller electrodes (1 mm diameter) are much more likely to give tritium than those which are larger, e.g., 4-6 mm diameter. The reason may come from the dendrite growth [5]. For successful tritium formation,

$$V_{sol} V_{met} C_o / \delta A > 1 \qquad (4)$$

Hence, the larger A, the greater must be the concentration of depositing ions to attain the condition indicated. Large electrodes will thus be less likely to show the phenomena.

Thus, with V_{sol} ~ 100 ccs, V_{met} = 8.8 ccs/mol, $C_o = 10^4$ moles L^{-1}, $\delta = 10^{-3}$, 5×10^{-3} M is sufficient impurity concentration. With r = 0.3 mm, the required impurity concentration is 6 times larger and unreasonably large impurity concentrations for switch on times ~ 100 days are necessary.

Finally, the factors which would likely increase Fleischmann-Pons effects are:

(1) Pd or alkaline solutions may not be necessary. The metal has to exhibit a Volmer-Heyrovsky path with coupled electrochemical desorption in rate control, because this mechnism of deuterium evolution gives surfaces completely covered with D at high current densities.

(2) Surfaces should be spiky. The tip radii should be minimal [22] . The promontories must grow for a time long enough to penetrate the diffusion layer of the flat electrode.

(3) Surface states should be promoted.

(4) Any method which causes the field in the double layer to fluctuate (e.g. heterodyne beats of superimposed a.c.) would be advantageous.

(5) The working region for D_2 evolution should be as far as possible negative to the electrode p.z.c. of the dendrite forming material.

The most needed information concerns the influence of Li, gas phase tritium production and He. X-ray and γ emission during the rare bursts should be sought.

CONCLUSIONS

(1) The Fleischmann-Pons effects (Heat and Tritium) have been observed in around one quarter of the electrodes used in the cathodic evolution of deuterium after very long times. The success rate improves greatly – up to 70% for T – if the electrode diameter is ~ 1 mm or less.

(2) Tritium reaches 10^4-10^7 disintegration min^{-1} ml^{-1} in the solution. Bursts of T last for c. 5-50 hours.

(3) The tritium increases to steady state concentration in solution over ~ 12 hours.

(4) There is a weak suggestion for some correlation between heat and tritium.

(5) The frequency with which the phenomena are observed falls as the electrode size increases. No effects have been observed when the electrode diameter exceeded 4 mm.

(6) The repeated formation of tritium from deuterium establishes the nuclear nature of the sporadic effects occurring. No non-nuclear explanation for the heat has yet been found [3].

(7) It is difficult to justify a fugacity of D in Pd of > 10^6 ats. Fusion within Pd is therefore unlikely.

(8) D^+ ions are made from D_2O in the double layer during dielectric breakdown which begins near tips of promontories of foreign material growing on the electrode surface. Reasonable numerical agreement with experiment arises if the effective mass of the proton is as small as 0.01 or the electric field at the dendrite tip is ~ 2×10^9 volts cm^{-1}, or some combination of reduced effective mass and enhanced field.

(9) The model explains the long delay times, the sporadicity and the size effects. It may explain the high branching ratio.

ACKNOWLEDGEMENT

We are grateful for financial support from the Electric Power Research Institute (EPRI), the Welch Foundation, and Texas A&M University.

REFERENCES

1. M. Fleischmann, S. Pons and M. Hawkins, J. Electroanal. Chem., 261. 301 (1989); err 263, 187 (1989).
2. S.E. Jones et al., Nature, 338, 737 (1989).
3. R.C. Kainthla, M. Szklarczyk, L. Kaba, G.H. Lin, O. Velev, N.J.C. Packham, J.C. Wass and J. O'M. Bockris, Int. J. Hydrogen Energy 14, 771 (1989).
4. N.J.C. Packham, K.L. Wolf, J.C. Wass, R.C. Kainthla and J.O'M. Bockris, J. Electroanal. Chem., 270. 451 (1989).
5. G.H. Lin, R.C. Kainthla, N.J.C. Packham, O. Velev, and J.O'M. Bockris, Int. J. Hydrogen Energy (in press).
6. F.J. Mayer, Proceedings of the Workshop on Cold Fusion Phenomena Santa Fe, NM, May 1989.
7. M. Gajda, D. Harley, J. Rafelski and M. Sawicki, Proceedings of the Workshop on Cold Fusion Phenomena, Santa Fe, NM., May 1989.
8. K. Nagamine et al., Proceedings of the DOE Workshop on Cold Fusion Phenomena, Santa Fe, (1989)
9. M. Rabinowitz and D.H. Worledge, Private Communication to G.H. Lin, September, 1989.
10. J. O'M. Bockris, G.H. Lin, and N.J.C. Packham, Fusion Technology (to be published).
11. O. Velev and R.C. Kainthla, submitted to Fusion Technology, March (1990).
12. J. O'M. Bockris, M.A. Genshaw and M. Fullenweider, Electrochimica Acta, 15 (1970) 47.
13. K.L. Wolf, N.J.C. Packham, D. Lawson, J. Shoemaker, F. Cheng and J.C. Wass., Proceedings of the Workshop on Cold Fusion Phenomena, Santa Fe, NM, May 1989.
14. P.K. Iyengar, Fifth International Conference on Emerging Nuclear Energy Systems (ICENES V), Karlsruhe, West Germany, July, 1989.
15. T. Mizuno, Private Communication to J.O'M. Bockris, October 1989.
16. W.A. Adams, E.E. Criddle, G. Jerkiewicz, B. E. Conway, V.S. Donepudi and J. Hebert, Proceedings of the Electrochemical Society Meeting, Hollywood, Florida, October 1989.
17. D.M. Kolb and C. Franke, Submitted to J. Appl. Phys. (1989).
18. M. Szklarczyk, R.C. Kainthla and J.O'M. Bockris, J. Electrochem. Soc, 136 (9). (1989) 2512.
19. W. Schmickler and E. Henderson, J. Phys. Chem., 85, (1986) 1.
20. Y.E. Kim, Proceedings of the First Annual Conference on Cold Fusion, Salt Lake City, UT, March 1990.
21. J.R. Oppenheimer and M. Philips, Phys. Rev., 48, (1935) 520.
22. J.L. Barton and J.O'M. Bockris, Proc. Roy. Soc, A268. (1962) 485.